

# Comparing numerical and analytical calculations of post-ISCO ringdown amplitudes

Shahar Hadar,<sup>1,\*</sup> Barak Kol,<sup>1,†</sup> Emanuele Berti,<sup>2,3,‡</sup> and Vitor Cardoso<sup>4,2,§</sup>

<sup>1</sup>*Racah Institute of Physics, Hebrew University, Jerusalem 91904, Israel.*

<sup>2</sup>*Department of Physics and Astronomy, The University of Mississippi, University, MS 38677, USA*

<sup>3</sup>*California Institute of Technology, Pasadena, CA 91109, USA*

<sup>4</sup>*CENTRA, Departamento de Física, Instituto Superior Técnico, Universidade Técnica de Lisboa - UTL, Av. Rovisco Pais 1, 1049 Lisboa, Portugal.*

(Dated: June 25, 2018)

We numerically compute the ringdown amplitudes following the plunge of a particle from the innermost stable circular orbit (ISCO) of a Schwarzschild black hole in the extreme-mass ratio limit. We show that the ringdown amplitudes computed in this way are in good agreement with a recent analytical calculation [1].

PACS numbers: 04.40.Dg, 04.62.+v, 95.30.Sf

## I. INTRODUCTION

In this paper we will study a compact object plunging into a much more massive, nonrotating (Schwarzschild) black hole from the innermost stable circular orbit (ISCO), located (in Schwarzschild coordinates) at  $r_{\text{ISCO}} = 3r_s$ , where  $r_s = 2M$  is the Schwarzschild radius and  $M$  is the black hole mass. This post-ISCO plunge trajectory is of special interest because it is “universal”. It has long been known [2] that the eccentricity of bodies orbiting a black hole must decrease in the Newtonian regime of low velocities and large separations ( $r \gg r_s$ ) during a gravitational-wave driven inspiral. In this sense, a plunge from a quasicircular ISCO represents a “Keplerian attractor”: for long, gravitational-wave driven inspirals the eccentricity should be essentially zero by the time the particle reaches the ISCO. However, some astrophysical scenarios do predict the possibility of orbits retaining nonzero eccentricity all the way down to plunge (see e.g. [3–6]).

This “universal” plunge trajectory for particles falling from a quasicircular ISCO leaves a very specific signature in the quasinormal ringing of the final black hole. The amplitudes of the quasinormal modes excited in the process were computed in Ref. [1]. In this paper we confirm the predictions of that paper by computing gravitational radiation with a frequency-domain perturbative code developed and tested in Ref. [8], and we verify that the two calculations are in very good agreement. Therefore any model for extreme mass ratio inspirals leading to plunge from a quasicircular ISCO should match the ringdown signal predicted in Ref. [1] at late times. It will be interesting to generalize the present results to comparable mass ratio binaries.

The paper is organized as follows. In section II we describe the post-ISCO plunge trajectory and the nu-

merical algorithm to compute the gravitational radiation produced by the plunging particle, along with the resulting waveforms. In section III we extract the ringdown amplitudes from these waveforms and present a comparison with the results of Ref. [1].

## II. RADIATION SOURCED BY INFALLING OBJECT

The post-ISCO plunge trajectory is described by the coordinates  $t, r, \phi$  as a function of the proper time  $\tau$  (without loss of generality we take the orbit to lie in the equatorial plane, i.e.  $\theta = \pi/2$ ). The trajectory is a solution of the geodesic equations

$$\tilde{E} = f(r) \frac{dt}{d\tau} \quad (1)$$

$$\tilde{L} = r^2 \frac{d\phi}{d\tau} \quad (2)$$

$$\tilde{E}^2 = \left( \frac{dr}{d\tau} \right)^2 + f(r)(\tilde{L}^2/r^2 + 1), \quad (3)$$

where  $f(r) = 1 - r_s/r$  and the energy and angular momentum per unit mass have the values corresponding to a particle at the ISCO:

$$\begin{aligned} \tilde{E} &= \tilde{E}_{\text{ISCO}} \equiv \frac{2\sqrt{2}}{3} \\ \tilde{L} &= \tilde{L}_{\text{ISCO}} \equiv \sqrt{3}r_s. \end{aligned} \quad (4)$$

The plunge trajectory can be written down analytically: cf. Eq. (2.7)–(2.11) and Fig. 1 of Ref. [1]. In perturbation theory, the gravitational radiation at infinity can be determined from a knowledge of the Sasaki-Nakamura wave function  $X_{lm}$  [7] (for the extensive literature on gravitational waves from particles falling into black holes, see [8, 9] and Appendix C of [10]). In the frequency domain, the Sasaki-Nakamura equation can be written in the form

$$\frac{d^2 X_{lm}}{dr_*^2} + \left[ \omega^2 - \frac{\Delta}{r^5} (l(l+1)r - 6M) \right] X_{lm} = S_{lm}. \quad (5)$$

\* shaharhadar@phys.huji.ac.il

† barak\_kol@phys.huji.ac.il

‡ berti@phy.olemiss.edu

§ vitor.cardoso@ist.utl.pt

Here  $(l, m)$  are (tensor) spherical harmonic indices resulting from a separation of the angular variables,  $\omega$  is the Fourier frequency of the perturbation and  $\Delta \equiv r(r-2M)$ . The boundary conditions dictate that we should have outgoing waves at infinity and ingoing waves at the BH horizon:

$$X_{lm} = \begin{cases} X_{lm}^{\text{in}} e^{-i\omega r_*}, & r_* \rightarrow -\infty, \\ X_{lm}^{\text{out}} e^{i\omega r_*}, & r_* \rightarrow +\infty. \end{cases} \quad (6)$$

The source term  $S_{lm}$  in the Sasaki-Nakamura equation (5) is determined by the point-particle trajectory, and it can be found in Ref. [8]. In terms of the Sasaki-Nakamura wavefunctions, the plus- and cross- polarization amplitudes are given by

$$h_+ + ih_\times = \sum_{lm} -2Y_{lm}(h_{+lm} + ih_{\times lm}) \quad (7)$$

$$= \frac{8}{r} \int_{-\infty}^{+\infty} d\omega \sum_{lm} e^{i\omega(r_*-t)} -2Y_{lm} X_{lm}^{\text{out}}. \quad (8)$$

In our comparisons we will always consider, for simplicity, the outgoing amplitudes of the Sasaki-Nakamura wavefunction in the time domain, i.e.

$$X_{lm}^{\text{out}}(t) \equiv \int_{-\infty}^{+\infty} d\omega e^{i\omega(r_*-t)} X_{lm}^{\text{out}}(\omega). \quad (9)$$

Numerically, the problem is to determine the (complex) amplitudes  $X_{lm}^{\text{out}}(t)$  for plunge trajectories with energy and angular momentum given by Eq. (4). In order to start the plunge, we must displace the particle from the ISCO location by a small quantity  $\epsilon$ :

$$r_0 = r_{\text{ISCO}}(1 - \epsilon). \quad (10)$$

We will present comparisons for  $\epsilon = 5 \times 10^{-3}$  and  $\epsilon = 10^{-2}$ , but we verified that our results are robust by computing the radiation for several other values of  $\epsilon$ , including  $\epsilon = 5 \times 10^{-4}, 10^{-3}, 5 \times 10^{-3}, 10^{-3}, 5 \times 10^{-3}, 10^{-2}$ .

Our numerical integrations use a modification of the C++ program described in Ref. [8], and we refer the reader to that paper for more details. All differential equations are integrated in C++ using the adaptive step-size integrator STEPPERDOPR5 [11]. First we integrate the solution of the homogeneous SN equation (5) with ingoing boundary conditions at the horizon from  $r_h = 2M(1 + \delta r)$  outwards (typically we choose  $\delta r = 10^{-4}$ ). Then we integrate the solution with outgoing boundary conditions at infinity from  $r_\infty = r_\infty^{(0)}/\omega$  inwards, where typically we choose  $r_\infty^{(0)} = 2 \times 10^3$ . From these two independent solutions we compute the Wronskian at the (large but finite) radius  $r_\infty^{(0)}$ . We integrate the geodesics with given orbital parameters, and at the same time we compute the source term corresponding to this trajectory. We output the solution with ingoing boundary conditions at the horizon  $X_{\text{in}}^{(0)}$  and the source term  $S_{lm}$  on three numerical grids (each consisting of  $n = 1.6 \times 10^5$  collocation points). The three grids cover the intervals

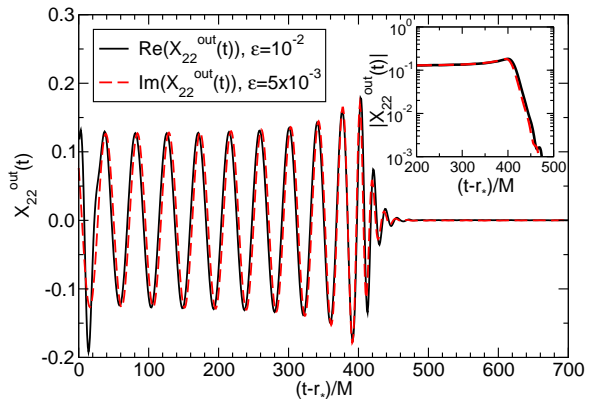


FIG. 1. Visual comparison of two waveforms for  $l = m = 2$  with differing cutoffs ( $\epsilon = 10^{-2}, 5 \times 10^{-3}$ ). The time axis has been shifted so that the maxima of the wave amplitudes  $|X_{lm}(t)|$  (shown in the inset) occur at the same value of  $(t - r_*)/M$ .

$[r_\infty, r_+]$ ,  $[r_{\text{ISCO}}, r_{\text{ISCO}} - 0.1]$  and  $[r_{\text{ISCO}} - 0.1, r_h]$ , respectively. This is necessary to keep good accuracy in the near-ISCO region, where the particle spends a lot of time when  $\epsilon$  is small. We use a Gauss-Legendre spectral integrator [11] to compute the convolution of  $X_{\text{in}}^{(0)}$  with the source term to find the outgoing wave amplitude  $X_{lm}^{\text{out}}(\omega)$ . Finally we sum over multipoles to get the total radiated energy, angular momentum and linear momentum, and we perform a Fourier transform to get  $X_{lm}^{\text{out}}(t)$ .

The real part of the  $l = m = 2$  waveforms for cutoff values  $\epsilon = 5 \times 10^{-3}$  and  $\epsilon = 10^{-2}$  are shown in Figure 1. This visual comparison shows quite clearly that the ringdown portion of the signal is very weakly dependent on  $\epsilon$ .

### III. EXTRACTING RINGDOWN AMPLITUDES FROM WAVEFORMS

In this section we describe the procedure we used to extract the ringdown amplitudes from the numerical waveforms and to compare with Ref. [1].

In the ringdown phase, the gravitational waveform is described by a superposition of quasinormal modes of the form

$$X_{lm} = \mathcal{N} \sum_{nlm} R_{nlm} \exp i\omega_{nlm}(t - t_0) \quad (11)$$

where we dropped the “out” superscript for simplicity. Here  $\omega_{nlm}$  are the (complex) characteristic ringdown frequencies,  $R_{nlm}$  are the amplitudes,  $\mathcal{N}$  is an overall normalization and  $t_0$  is a time shift which determines the origin of time. We stress that while some readers may be more familiar with the odd and even radiation functions  $\psi_{lm}^{(\text{odd})}$  (Regge-Wheeler) and  $\psi_{lm}^{(\text{even})}$  (Zerilli), here we work with the Sasaki-Nakamura radiation functions  $X_{lm}$ , which do not have a specific parity.

Given a numerical time-domain waveform  $X_{lm}(t)$ , our objective is to extract the amplitudes  $R_{nlm}$ . The leading amplitude ( $n = 1$ ) is extracted by plotting  $\log|X_{lm}|$  as a function of  $t$  (see the inset of Figure 1). At late times only the dominant mode contributes to the signal, and  $\log|X_{lm}|$  becomes a linear function of time with slope given by the decay constant  $\gamma_1 \equiv \Im(\omega_{1lm})$ . The intercept is exactly the desired amplitude,  $\log|R_{1lm}|$ . The discrepancy between the expected and measured  $\gamma_1$  contributes to the error estimate for  $|R_{1lm}|$ . In practice, this contribution is minimized if the origin of time is close to the center of the linear portion in the curve.

In the same fashion one can extract the amplitude of the second overtone, namely  $|R_{2lm}|$ . In preparation for this, one should first extract the phase of  $R_{1lm}$ . This is done by plotting  $X'_{lm} = X_{lm} \cdot \exp(\gamma_{1lm}t)$  as a function of  $t$ , so that  $X' \simeq R \exp(i\Re(\omega_{1lm})t)$  should be a periodic function with frequency  $\Re(\omega_{1lm})$  and complex amplitude  $R_{1lm}$ . Once we know the (complex) amplitude  $R_{1lm}$ , we can subtract the dominant ringdown mode to obtain a residual  $X_{lm}^{(2)}(t) = X_{lm}(t) - R_{1lm} \exp(i\omega_{1lm}t)$ . Now we can repeat the steps above to find the amplitude of the second overtone. Indeed, the procedure can be repeated for generic overtone numbers  $n$  as long as the signal is not dominated by numerical noise, i.e., as long as the residuals  $X_{lm}^{(n)}$  exhibit a decaying exponential behavior.

The value of the amplitudes depends, in principle, on the constants  $\mathcal{N}, t_0$ . To sidestep this difficulty we compute the discrepancy of each mode

$$\Delta \equiv \log \left( R_{nlm}^{\text{analyt}} / R_{nlm}^{\text{num}} \right), \quad (12)$$

where  $R_{nlm}^{\text{analyt}}$  is the ‘‘analytical’’ amplitude computed in Ref. [1] and  $R_{nlm}^{\text{num}}$  is the numerically extracted amplitude. Next we plot  $\Delta$  as a function of the mode decay constant  $\gamma_{nlm}$ . Clearly a rescaling by  $\mathcal{N}$  will shift  $\Delta$  by a constant, while a shift of  $t_0$  corresponds to a change in slope. In particular, for modes with identical decay constants (such as modes with different  $m$  and fixed  $l$ ) the discrepancy  $\Delta$  is the same and it is independent of  $t_0$ . Now we can carry out a linear fit of  $\Delta_{nlm} = \Delta_{nlm}(\gamma_{nlm})$ . This fit will yield the constants  $\mathcal{N}, t_0$  required for the amplitudes to agree, i.e.,  $R_{nlm}^{\text{analyt}} = R_{nlm}^{\text{num}}$ . The origin of time resulting from the linear fit was compared to the conventions of Ref. [1], where it was chosen such that  $r(t=0) = 1.1r_s$ . We found that the same happens here

to a good approximation.

We performed comparisons for 16 different modes with the following  $(nlm)$  values (for  $\epsilon = 0.005$ ): the modes  $2 \leq l \leq 4$  for  $0 \leq m \leq l$  and  $l = 5$  for  $2 \leq m \leq 5$ , all with  $n = 1$ .

Our main results are shown in Figure 2. After the linear fit, the residual errors are seen to be of  $\sim 1\%$ . We also performed the comparison for the mode  $(nlm) = (222)$  (second overtone of  $l = m = 2$ ). In this case we found good agreement up to a residual error of  $\sim 10\%$ , consistent with our error estimate for the numerically extracted amplitude in this case. A similar comparison was made also for  $\epsilon = 0.01$  for some modes, and good agreement was found - up to an overall estimated error of  $\sim 1\%$ .

In summary, for all the tested modes (see the list above) the numerical amplitudes here were found to coincide with the analytic ones computed in [1].

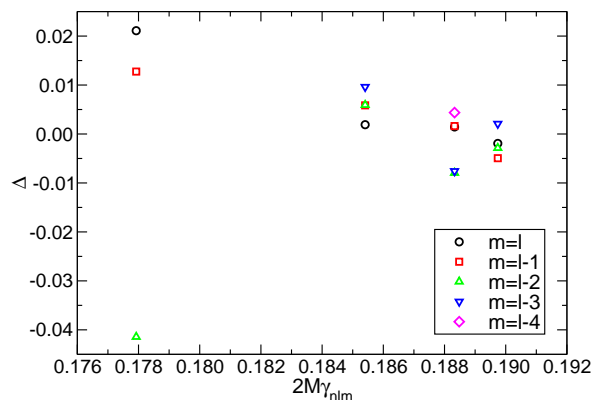


FIG. 2. Amplitude comparison for 16 different modes with  $n = 1$  and  $\epsilon = 5 \times 10^{-3}$ . The horizontal axis represents the decay constant  $\gamma_{nlm}$  in units where  $r_s = 1$ . Each point represents the residual  $\Delta$  value (after subtracting a linear fit or tuning  $\mathcal{N}, t_0$ ) for the given  $(l, m)$ . Different  $\gamma_{nlm}$  values correspond to different  $l$ 's: the leftmost points correspond to  $l = 2$ , and  $\gamma_{nlm}$  grows monotonically with  $l$ .

*Acknowledgements:* This work was supported by the *DyBHo-256667* ERC Starting Grant, NSF PHY-090003 and FCT - Portugal through PTDC projects FIS/098025/2008, FIS/098032/2008, CTE-AST/098034/2008, and CERN/FP/109290/2009. E.B.'s research was supported by NSF Grant No. PHY-0900735.

[1] S. Hadar, B. Kol, [arXiv:0911.3899 [gr-qc]].  
 [2] P. C. Peters, Phys. Rev. **136**, B1224 (1964).  
 [3] L. Barack and C. Cutler, parameter estimation accuracy,” Phys. Rev. **D69**, 082005 (2004) [arXiv:gr-qc/0310125].  
 [4] C. Hopman and T. Alexander, black hole: Characterizing gravitational wave sources,” Astrophys. J. **629**, 362 (2005) [arXiv:astro-ph/0503672].

[5] P. Amaro-Seoane, J. R. Gair, M. Freitag, M. Coleman Miller, I. Mandel, C. J. Cutler and S. Babak, Class. Quant. Grav. **24**, R113 (2007) [arXiv:astro-ph/0703495].  
 [6] N. Yunes, K. G. Arun, E. Berti, C. M. Will, Phys. Rev. **D80**, 084001 (2009). [arXiv:0906.0313 [gr-qc]].  
 [7] M. Sasaki and T. Nakamura, Phys. Lett. A **89**, 68 (1982). M. Sasaki and T. Nakamura, Prog. Theor. Phys. **67**, 1788 (1982).

- [8] E. Berti, V. Cardoso, T. Hinderer *et al.*, Phys. Rev. **D81**, 104048 (2010). [arXiv:1003.0812 [gr-qc]].
- [9] T. Nakamura, K. Oohara, Y. Kojima, Prog. Theor. Phys. Suppl. **90**, 1-218 (1987).
- [10] E. Berti, V. Cardoso, J. A. Gonzalez *et al.*, Phys. Rev. **D76**, 064034 (2007). [gr-qc/0703053 [GR-QC]].
- [11] W. H. Press, S. A. Teukolsky, W. T. Vetterling, and B. P. Flannery, *Numerical Recipes in C++ - The Art of Scientific Computing - Third Edition*(Cambridge University Press, Cambridge, England, 2007).